Updated version 1.1

Magnetic attraction forces on ferromagnetic particles

Metal powder sticking on a connecting rod screw

Metal swarf sticking on a bearing cylinder roller

Metal powder sticking on a bearing cylinder roller

Maurer Magnetic AG
8627 Grüningen
Switzerland

 © Maurer Magnetic AG 03.2015

Maurer Magnetic AG, your specialist for:

- Industrial demagnetizing devices and systems
- Instruments for measuring magnetic fields
- Degaussing services

© Maurer Magnetic AG 03.2015

Abstract

Particles are known as cause of errors in the production, the assembly and the operation of high quality products. For this reason, expensive methods are used to keep the particle contamination as low as possible. Accordingly, a cleanliness trend in the automotive OEM and supplier industry can be observed. Other industries start to follow this trend and are increasingly adopting the standards and technologies from the automotive companies.

The main interest in residual dirt contamination risk assessments lies with hard, metal particles, generally because they have the greatest potential for faults in manufacturing processes and in the final product.

Some examples:

- Cleaning equipments can not reliably remove metal particles.
- Machining processes are affected by chips sticking to tools and parts.
- Surface coatings adhere poorly or flake off due to contamination of the base material.
- The quality of painted surfaces is poor due to particle buildup at corners and in narrowings.
- Powder metallurgy, fine blanking or stamping processes are affected by adhesion of sinter powder or punching residues.
- Particles created by cracked connecting rods prevent the subsequent precise assembly.
- Electrically conductive particles cause short circuits on electronic circuits.
- Hard particles clinging to sliding or roller bearings lead to premature failure of the final product.
- Metal shavings inside of hydraulic blocks may cause malfunction of valves.
- Gasoline or diesel injection systems may be damaged by critical particles.

Wherever magnetic adhesion of metal chips or particles plays a role, an significant improvement in subsequent cleanliness sensitive processes (e.g. parts cleaning, coating...) is achieved by demagnetization.

Summary

With respect to the magnetic attraction potential, metal particles can be divided in magnetic (ferromagnetic behavior) and nonmagnetic particles.

The magnetic attraction force on ferromagnetic particles is proportional to the field gradient and the absolute field strength acting on the particle. According to the Automotive Industry Standard VDA19 / ISO16232 particle sizes down to 5 microns are considered here.

The minimum distance between the active measurement zone to the surface of the parts is limited by the size of the Hall sensor of residual magnetism measuring devices. This distance is approximately 0.5mm (500µm). Many magnetic field measuring instruments used in industrial companies exhibit a significantly larger distance of the active measuring zone.

The residual magnetism distribution on ferromagnetic parts is usually of fine pole and chaotic nature. The variation of field strength takes place within small distances, which leads to large field gradients in the surface vicinity.

This paper introduces a physical calculation model that is compared with practical experiments, in order to gain knowledge about magnetic field gradients, field strengths and finally, magnetic attraction forces on ferromagnetic particles.

Magnetization of ferromagnetic particles

The magnetic properties of metal particles depend on whether they behave paramagnetic, diamagnetic or ferromagnetic. Paramagnetic (e.g. austenitic stainless steel) or diamagnetic (e.g. aluminum) particles can't be attracted by field strength in the usual order of residual magnetism (about 0 ... 60 Gauss).

Ferromagnetic particles can however, due to the high magnetic susceptibility even at low field strengths, magnetize significantly and remain attached on ferromagnetic components.

Calculation of the magnetic attraction force on particles

The magnetic susceptibility χ describes the magnetization of a material. The susceptibility χ_p of a particle is calculated according to [1]:

$$M_p = \frac{(\mu_i H_p)}{\left(1 + \mu_i H_p / M_s\right)} \quad \text{and} \quad \chi_p = M_p / H_p$$

H_p [A/m] is the magnetic field strength acting in the center of gravity of the particle.

The magnetic susceptibility χ_p = 20 ... 36 of spherical iron particles is calculated by formula [1] and the values: saturation magnetization M_s = 1550 [kA/m], relative permeability μ_i = 40 and field strength H_p between. 1 ... 50 [A/cm].

M_p is the magnetization of the particle.

The magnetic attraction force on ferromagnetic particles is calculated by [2]:

$$\mathbf{M_p} = \chi_p \mathbf{H_p} \quad \text{and} \quad \mathbf{F_m} = \mu_0 V_p \mathbf{M_p} \nabla(\mathbf{H_p})$$

$\mathbf{F}_m$ magnetic attraction force on particle [N]

μ_0 = 1.256x10^{-6}, permeability of vacuum [Vs/Am]

V_p particle volume [m^3]. $V_p \sim d_p^3$

$\nabla(\mathbf{H}_p)$ field gradient[1] in center of gravity of the particle [A/m^2].

The field strength and the field gradient are assumed acting in the center of gravity of the particle for simplicity reasons. The particle shape is modeled as a sphere. The distance of the center of gravity to the surface of the sphere is thus $d_p/2$ of the particle. The volume V_p results from V_p = 4/3 * Pi * $(d_p/2)^3$.

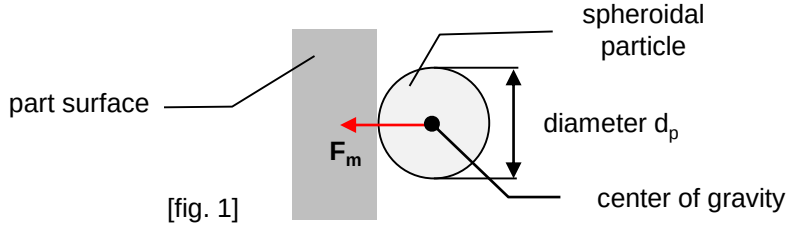

[fig. 1]

[1]field gradient = measure of field intensity change per unit distance

Estimation of field strength and field gradient in the surface vicinity

Residual magnetism below ~0.5mm distance to the surface can no longer be measured, because of the housing size of Hall sensors. Field strength and field gradient in the center of gravity of a particle with diameter d_p smaller than 0.5mm must be calculated therefore by a mathematical model.

A magnetized region on the surface [fig. 2, 3, 4] is approximated by a dipole magnetized cylinder [fig. 5]. The dimensions h, r, and the magnetization M of the cylinder determine the field strength along the z-axis at the center of the cylinder. The field strength is calculated at a distance Z_0 from the surface of the cylinder. By using experimentally determined parameters h, r and M, field profiles consistent with measured values can be found along the Z-axis. This allows the estimation of the required field strength and field gradient in order to calculate the magnetic attraction force on particles with a diameter smaller than 500µm.

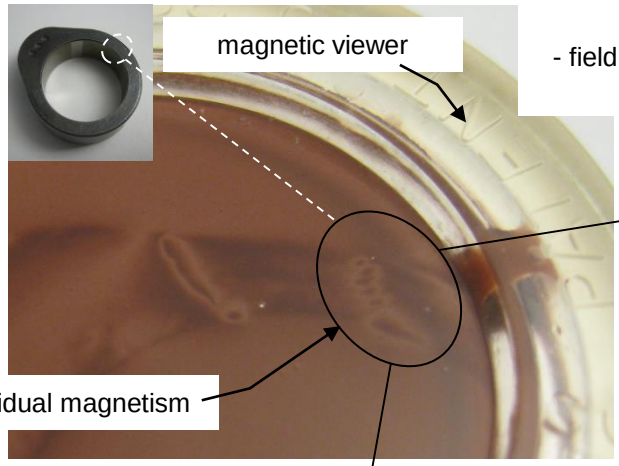

[fig. 2]

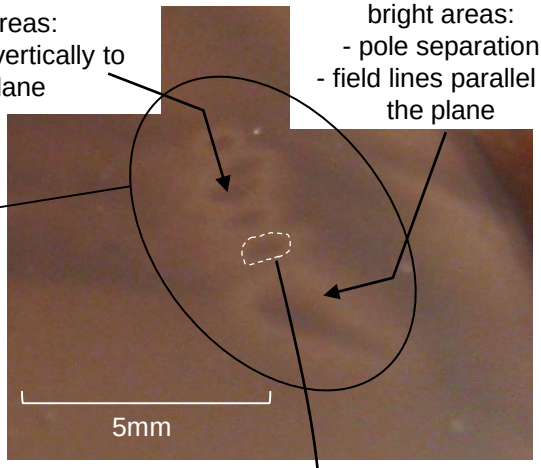

[fig. 3]

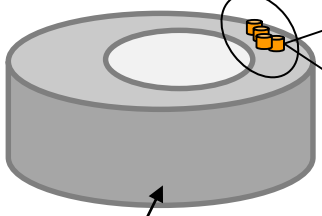

[fig. 4]

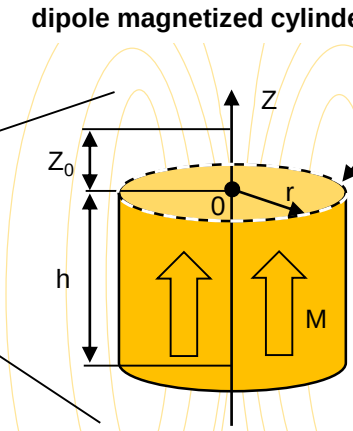

[fig. 5]

field lines

Field profile of a magnetized cylinder along the Z-axis

The field strength H is calculated acc. to. [3]:

$$H(Z_0) = 2\pi M\left[\frac{Z_0 + h}{\sqrt{(Z_0 + h)^2 + r^2}} - \frac{Z_0}{\sqrt{{Z_0}^2 + r^2}}\right]$$

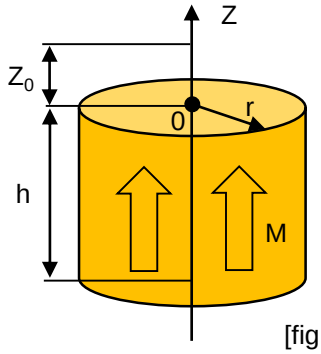

[fig. 6]

Field profile of different cylinders

To evaluate the field distribution in response to the cylinder size, three examples were calculated with different parameters.

The field profile of the cylinder with h=1, r=0.5, curve H1(Z0), corresponds to a magnetic spot on the surface of a ferromagnetic component, created by a magnetized screwdriver tip.

The magnetization with a screwdriver tip was chosen to represent a realistic case. Fine pole magnetizations correspond to this case in the trend.

field profile parameters

	H1(Z0)	H2(Z0)	H3(Z0)
h [mm]	1	2	3
r [mm]	0.5	1.0	1.5
M [A/m]	240	240	240

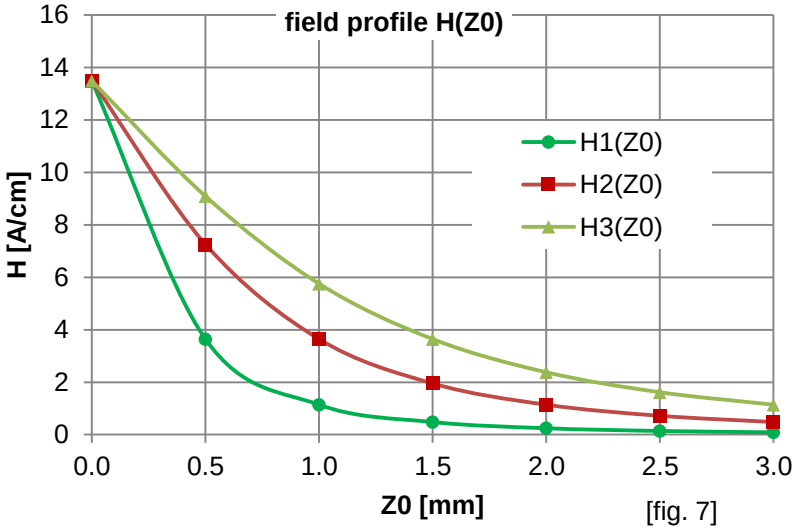

[fig. 7]

Field gradient in the vicinity of the surface

The field strength is declining increasingly for cylinders with smaller values of h and r [fig. 7]. Parts with chaotic, fine pole residual magnetism follow the same trend and have a limited range of the magnetic stray field.

The field gradient is accordingly higher for smaller cylinders and also higher for increasingly fine pole residual magnetism on the part surface.

© Maurer Magnetic AG 03.2015

Magnetic attraction force compared to the weight force

The magnetic attraction force F_m is compared in this practical test in relation to the weight force F_g of the particle.

Van der Waals forces are neglected in the consideration and electrostatic effects do not occur due to the electrical conductivity of the metal parts and particles. Liquid or solid bridges are eliminated in the experiments.

The residual magnetism is experimentally applied with a magnetized tip (cross screwdriver) on a 100Cr6 cylinder roller [fig. 10]. The magnitude of the residual magnetism point is experimentally set in a way, that a ferromagnetic particle nearly remains stick with its weight force.

In such case, approximately the equation: $F_m = F_g$ applies.

The field profile [fig. 11] causing the particle adhesion is used for subsequent comparison of the attraction force calculation with the experiment. The field profile and the attraction experiment were determined in the center area of the residual magnetism spot.

Elongated particle [fig. 8]
The magnetization increases with a slenderness ratio L:D ~ 5:1 by a factor of 1.44, compared to a spherical particle (acc. to [4]).

Spherical particle [fig. 9]
The particle shape (sintered powder) is approximately spherical.
To be noted is the formation of particle strings along the field lines.
The length of the particle strings is approximately equal to the 1000µm elongate particle.

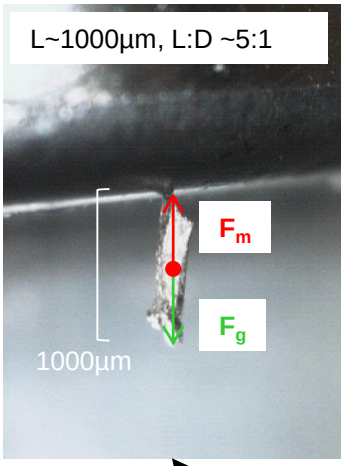

[fig. 8]

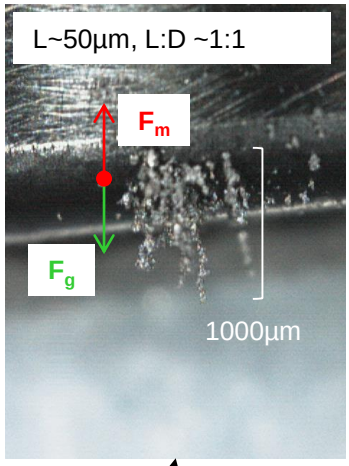

[fig. 9]

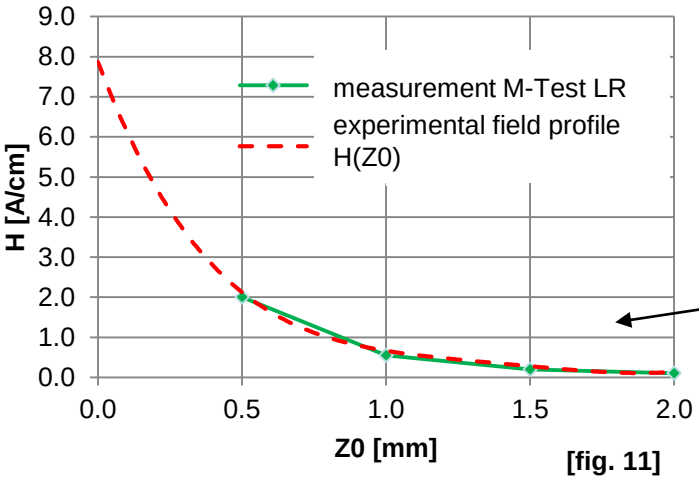

[fig. 11]

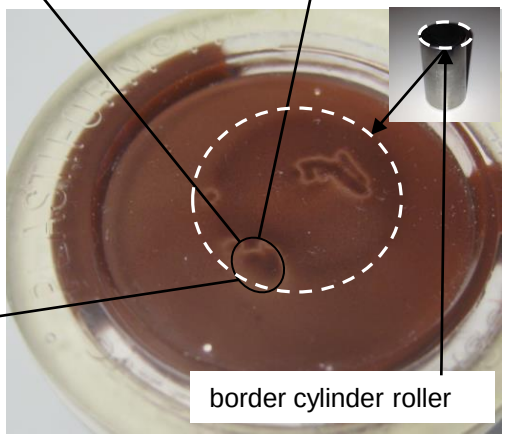

[fig. 10]

Correction factor for directional measurement of the magnetic field

Most industrial field strength meters use probes with a single Hall element. Triaxial Hall sensors are too large and will lead to a substantially larger measuring distance from the surface. They are therefore less suitable for residual magnetism measuring instruments.

The field strength is measured by directional measuring instruments (e.g. M-Test LR / LL) therefore only in one axial direction. Acc. to [fig. 12], the active Hall zone is fluxed perpendicularly to H_z. The reading corresponds in consequence to H_z. Field strength as a vectorial size has three spatial components of the field strength: $\mathbf{H} = H_x+H_y+H_z$.

The magnitude of the vector is calculated according to.: $|\mathbf{H}| = \sqrt{H_x^2 + H_y^2 + H_z^2}$

A simplifying assumption is made for residual magnetism of small spatial extent (dimension Hall sensor ~ dim. cylinder). All three directions provide the same contribution, it follows upon knowledge of H_z:

$$|\mathbf{H}| = \sqrt{3H_z^2} = \sqrt{3}H_z$$

The result is a correction factor $\sqrt{3}$. To obtain the field vector **H** out of the normal vector component H_z, the assumption is justified to multiply the value H_z by the factor $\sqrt{3}$.

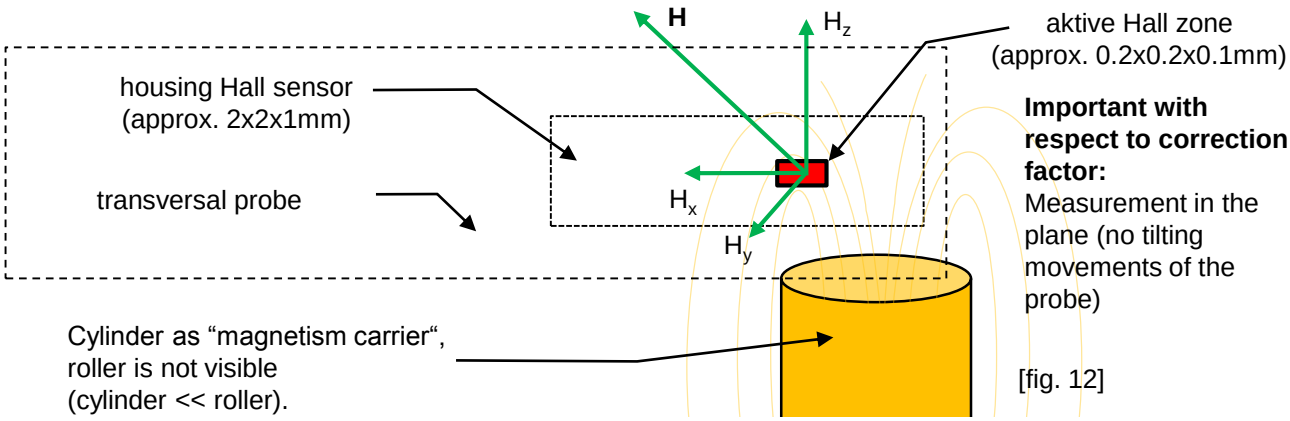

[fig. 12]

Field strength acting on particle

The scaling of the field profile of [fig. 11] with the correction factor $\sqrt{3}$ leads to the field profile according to [fig. 13]. The attraction force calculation is done with the scaled field profile.

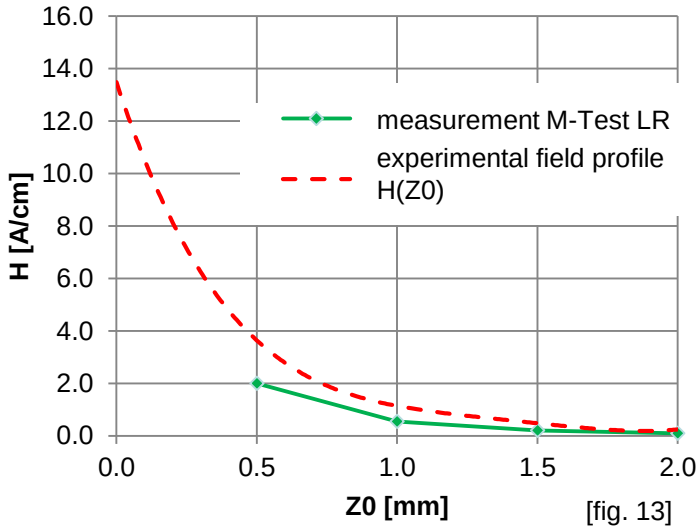

[fig. 13]

Calculation of magnetic attraction

The magnetic attraction force on particles is calculated by using the methods of the previous pages and compared with the experimental results.

Field gradient

The field gradient acc. to [fig. 14] is calculated by behalf of the field profile H(z). Near the zero point a flattening of the field gradient is observed. This behavior results in the vicinity: $Z_0 << h, r$.

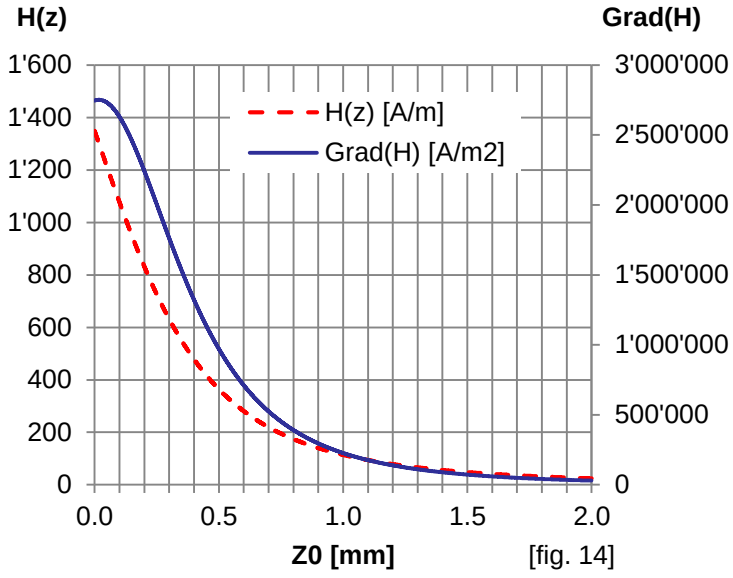

[fig. 14]

Calculation of the attraction forces assuming the following parameters

param.	value	notes
h [mm]	1	acc. to page 6
r [mm]	0.5	acc. to page 6
M [A/m]	240	acc. to page 6
m_{spec} [kg/m³]	7‘800	spec. mass
χ_{p1}	25	suscep. particle 50µm, L:D ~1:1, acc. to page 4
χ_{p2}	36	suscep. particle 1000µm, L:D ~5:1, acc. to page 4

Comparision calculation / experiment

50µm particle acc. to [p. 7, fig. 9]
The spherical particles stick acc. to [fig. 15] with a ratio Fm/Fg ~1.44. This order of magnitude seems plausible in comparison with the experiment of page 7.

1000µm particle acc. to [p. 7, fig. 8]
The elongated 1000µm particle from page 7 has approximately a 13-fold lower weight compared to spherical particle. From [fig. 15] follows for a spherical particle of diameter 1000µm, Fm/Fg ~0.21.
For a 13-fold lower weight force follows Fm/Fg ~ 2.73. These adhesive force seems plausible in comparison with the experiment.

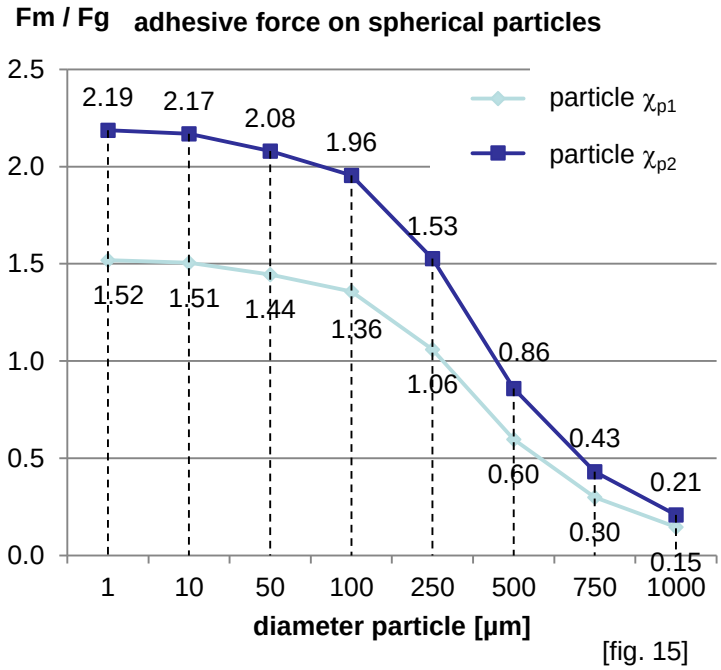

[fig. 15]

Findings

- Due to the housing size of Hall sensors, fine pole residual magnetism can't be measured correctly in a distance closer than 0.5mm from the surface. The field strength acting on small particles increases disproportionately the closer they are to the surface.
- The magnetic attractive force F_m on ferromagnetic particles grows with increasingly fine pole residual magnetism. The reason is the growing field gradient.
- The magnetic attraction force is bigger for a given residual magnetism acting on smaller particles, because of the increasing field strength and field gradient in the surface vicinity .
- Projecting edges lead to greatly increased field gradients and consequently high (approximately up to 100-fold greater) attractive forces on ferromagnetic particles.
- Halving the residual magnetism of the part leads to an approximately 4-times lower magnetic attracting force on particles ($F_m \sim H^2$).
- The magnetic attraction force F_m on particles grows within homogeneous field in the same way as the gravitational force F_g, proportionally to the cube of the particle diameter d_p. F_m , $F_g \sim d_p^3$.
- Slim particles are attracted more strongly than spherical particles at a given residual magnetism .
- The removal of particles or small parts by magnets doesn't work on ferromagnetic surfaces reliably, because the stray field of the magnet magnetizes also the area underneath the particle. Depending on the particular configuration (e.g. particles on edges) a stronger attraction force between particle and surface may result due to the high field strength and the high field gradient between particle and surface.
- The magnetic adhesion of particles can be minimized only by a complete demagnetization of the parts.

Literature

[1] A. Merino-Martos, J. de Vicente, L. Cruz-Pizarro, I de Vicente, 2011. „Setting up High Gradient Magnetic Separation for combating eutrophication of inland waters

[2] Mathias Stolarski, 2011. „Die Magnetfeldüberlagerte Zentrifugation, Ein neues hybrides Trennverfahren zur Selektiven Bioseparation"

[3] NT-MDT „ http://www.ntmdt.com/spm-basics/view/magnetic-field-cylinder-domens" , 07.03.2012

[4] Herbert Daniel, 1997 „Physik 2, Elektrodynamik, relativistische Physik", Seite 77